High-energy limit and internal symmetries

G. M. Cicuta and D. Gerundino
Istituto Nazionale di Fisica Nucleare, Sezione di Milano
and Istituto di Scienze Fisiche, Università di Milano Via Celoria 16,20123 Milano, Italy
(Received 18 April 1983)

In a model with global SU(N) invariance with a scalar field that transforms as the (N^2-1)-dimensional representation (symmetric adjoint) and interacts with cubic coupling, we study Regge poles and Regge cuts. The interplay between Regge behavior and the group of internal symmetry is analyzed with care.

I. INTRODUCTION

Non-Abelian global groups of symmetries and even more the non-Abelian local (gauge) symmetries play a dominant role in the current revival of quantum field theory as an essential part of our understanding of elementary particle physics. The bound-state properties and the high-energy behavior in these models are a difficult problem which is only partially understood.

The traditional logic used in the past of studying the Bethe-Salpeter equation in some weak-coupling approximation for the kernel (or some gauge-invariant approximation), or the leading-log energy graphs in the Regge limit, is debatable until a better understanding of confinement will be reached.

The leading-log energy approximation in the Regge limit (large energy, fixed momentum transfer) is itself very complex in non-Abelian gauge theories and the results obtained do not match the general understanding reached in the simple scalar cubic self-interaction. This is due mainly to the large number of Feynman graphs relevant at high order in perturbation theory, each of them being of difficult evaluation, and to the frequent cancellations among leading contributions.

In this work we solve a much simpler problem: the high-energy behavior of a scalar field with cubic self-interaction, the field transforming as the adjoint representation of SU(N). That is, the Lagrangian studied here is

$$\mathscr{L}(\phi)=\tfrac{1}{2}\,\mathrm{Tr}(\partial_\mu\phi\partial^\mu\phi-m^2\phi^2)+g\,\mathrm{Tr}(\phi^3)\ , \tag{1.1}$$

$$\phi\equiv\phi^i\lambda^i,\quad i=1,2,\ldots,N^2-1$$

$$\lambda^i\lambda^j\equiv\frac{4a}{N}\delta_{ij}I+(d_{ijk}+if_{ijk})\lambda^k\ , \tag{1.2}$$

$$\mathrm{Tr}(\lambda^i\lambda^j)=4a\delta_{ij},\quad \mathrm{Tr}(\phi^3)=4ad_{ijk}\phi^i\phi^j\phi^k\ . \tag{1.3}$$

λ_i are the usual generalizations to the SU(N) group of the Gell-Mann λ matrices for SU(3); d_{ijk} is a totally symmetric tensor, f_{ijk} is a totally antisymmetric tensor; a is an arbitrary normalization, and N is a positive integer larger than 2.

Since the space-time part of each Feynman graph in this model is the same as that of the well-studied ϕ^3 model (without internal symmetry), it may be considered as known and only the group-theoretic contributions are new. Finding the high-energy behavior of the simplest theory with non-Abelian global internal symmetry may (or may not) be suggestive for the far more difficult problem in a non-Abelian gauge theory. However, we find that the picture of Regge poles, Regge cuts, and Gribov calculus in our simple model is itself interesting.

We compute the group-theoretic contributions of the relevant Feynman graphs at every order in perturbation theory. This leads to the definition of a set of basis tensors called projectors, described in Sec. II. It is likely that the techniques described in this work may be useful in many problems where one computes the group weight of graphs in an arbitrary order. Furthermore for generality we computed in Sec. III the group weight of a class of graphs much larger than those needed in the present work. This is useful for the study of simple hybrid models where Regge poles have different symmetry than the present ones.

The group-theoretic factors computed in this paper may also be useful for theories with different interactions that can be recast in form similar to (1.3). For instance, consider the SU(N)-invariant Lagrangian with quartic interaction:

$$\mathscr{L}(\phi)=\tfrac{1}{2}\,\mathrm{Tr}(\partial_\mu\phi\partial^\mu\phi-m^2\phi^2)-\alpha^2\mathrm{Tr}(\phi^4)\ ,$$
$$\phi\equiv\phi^i\lambda^i,\quad i=1,2,\ldots,N^2-1 \tag{1.4}$$

$$\mathrm{Tr}(\phi^4)=\frac{16a^2}{N^2}(\phi^i\phi^i)^2+4ad_{ijk}d_{klm}\phi^i\phi^j\phi^l\phi^m\ . \tag{1.5}$$

After the introduction of a singlet auxiliary field σ and a set of auxiliary fields σ^h transforming as the adjoint representation of SU(N) one has

$$\mathscr{L}(\phi)=\tfrac{1}{2}\,\mathrm{Tr}(\partial_\mu\phi\partial^\mu\phi)-\frac{32a^2\alpha^2}{N^2}\left[\phi^i\phi^i\sigma-\frac{\sigma^2}{2}\right]$$
$$-8a\alpha^2\left[d_{ijh}\phi^i\phi^j\sigma^h-\frac{\sigma^k\sigma^k}{2}\right]\ , \tag{1.6}$$

where the cubic interaction among fields in the adjoint representation has the form of Eq. (1.1).

Finally we warn the reader that although the evaluation of group-theoretic factors is a straightforward exercise of trivial algebra, the time required increases rapidly with the

complexity of the graph; while the ladder in Sec. II only takes a few minutes, many results quoted in Sec. III take a few days.

The Regge poles of the model are described in Sec. II, while the convolution of a pair of Regge poles thus originating in the simplest form of Regge cut is described in Sec. III. Our conclusions, with brief comments on the analogous high-energy structures in non-Abelian gauge models, are summarized in Sec. IV.

II. BASIS TENSORS AND REGGE POLES

Every Feynman graph G factorizes into $W_G M_G$, where M_G is the space-time factor and W_G is the group-theoretic factor consisting in a product of various d_{abc} associated with the vertices of the graph and factors δ_{ab} for each internal line. The group-theoretic factor W_G may itself be considered a "Feynman integral" over a discrete finite space.[1]

The group factor of each Feynman graph that contributes to the elastic scattering amplitude is a rank-four tensor W_{abcd}. Its "evaluation" consists of expressing it as a linear combination of a set of (linearly independent) basis tensors B^i_{abcd}. The choice of the basis has some arbitrariness. Two choices are described here: the "natural" basis given by traces of four generators T_i and the projector basis. We follow the method of Cvitanović of evaluating W_G by first reexpressing all vertices d_{abc} in terms of the defining representation

$$d_{abc}=\frac{1}{8a}\mathrm{Tr}(\lambda^a\lambda^b\lambda^c+\lambda^c\lambda^b\lambda^a)\ , \tag{2.1}$$

then eliminating all internal lines associated with particles in the adjoint representation:

$$\frac{1}{4a}(\lambda^a)^i_j(\lambda^a)^k_l=\delta^i_l\delta^k_j-\frac{1}{N}\delta^i_j\delta^k_l\ ,$$
$$i,j,k,l=1,2,\ldots,N\ . \tag{2.2}$$

The group factor W_G is then expressed in terms of the "natural" basis, which are tensors where the steps 1 and 2 cannot further operate (analogous tensors of arbitrary rank are described in Fig. 21 of Ref. 1). The "natural" basis for rank-four tensors is made by a set of six tensors we label A, B, C, D, E, and F, represented in Fig. 1 (see Ref. 2):

$$\begin{aligned}
A_{abcd}&=\tfrac{1}{32}[\mathrm{Tr}(\lambda_a\lambda_d\lambda_c\lambda_b)+\mathrm{Tr}(\lambda_a\lambda_b\lambda_c\lambda_d)]\ ,\\
B_{abcd}&=\tfrac{1}{32}[\mathrm{Tr}(\lambda_a\lambda_b\lambda_d\lambda_c)+\mathrm{Tr}(\lambda_a\lambda_c\lambda_d\lambda_b)]\ ,\\
C_{abcd}&=\tfrac{1}{32}[\mathrm{Tr}(\lambda_a\lambda_d\lambda_b\lambda_c)+\mathrm{Tr}(\lambda_a\lambda_c\lambda_b\lambda_d)]\ ,\\
D_{abcd}&=a^2\delta_{ab}\delta_{cd}\ ,\\
E_{abcd}&=a^2\delta_{ac}\delta_{bd}\ ,\\
F_{abcd}&=a^2\delta_{ad}\delta_{bc}\ .
\end{aligned} \tag{2.3}$$

We call this basis natural because it presents itself as a natural instrument in the computation of a group weight. The other relevant basis we need is the "projector" basis which is the relevant basis to express the physics properties. Each projector is a tensor that corresponds to one irreducible representation of SU(N), then it describes a state of "pure quantum numbers" in a given channel. The "incoming" two-particle state transforms as the product of two symmetric (N^2-1)-dimensional representations which decompose in six irreducible representations, two of them antisymmetric and four symmetric ones:[3]

$$\begin{aligned}
(N^2-1)_S\otimes(N^2-1)_S=1_s\oplus(N^2-1)_A\oplus(N^2-1)_S\otimes&\left[\frac{(N^2-4)(N^2-1)}{4}+\overline{\frac{(N^2-4)(N^2-1)}{4}}\right]_A\\
\oplus\left[\frac{N^2(N-1)(N+3)}{4}\right]_S\oplus&\left[\frac{N^2(N+1)(N-3)}{4}\right]_S\ .
\end{aligned} \tag{2.4}$$

The six projectors which represent states with pure quantum number in the "t channel" (the vertical channel) are related to the "natural" basis by the following:[4]

$$\begin{aligned}
P_1\equiv P_{(1)}&=\frac{1}{a^2}\frac{1}{N^2-1}E\ ,\\
P_2\equiv P_{(N^2-1)_A}&=\frac{1}{a^2}\frac{1}{N}(B-C)\ ,\\
P_3\equiv P_{(N^2-1)_S}&=\frac{1}{a^2}\frac{N}{N^2-4}\left[(B+C)-\frac{2}{N}E\right]\ ,\\
P_4\equiv P_{[(N^2-4)(N^2-1)/4+\overline{(N^2-4)(N^2-1)/4}]_A}&=\frac{1}{a^2}\left[-\frac{1}{N}(B-C)+\frac{D-F}{2}\right]\ ,\\
P_5\equiv P_{[N^2(N-1)(N+3)/4]_S}&=\frac{1}{a^2}\left[\tfrac{1}{2}A-\frac{(B+C)}{2(N+2)}+\tfrac{1}{4}(D+F)+\frac{E}{2(N+1)(N+2)}\right]\ ,\\
P_6\equiv P_{[N^2(N+1)(N-3)/4]_S}&=\frac{1}{a^2}\left[-\tfrac{1}{2}A-\frac{(B+C)}{2(N-2)}+\tfrac{1}{4}(D+F)+\frac{E}{2(N-1)(N-2)}\right]\ .
\end{aligned} \tag{2.5}$$

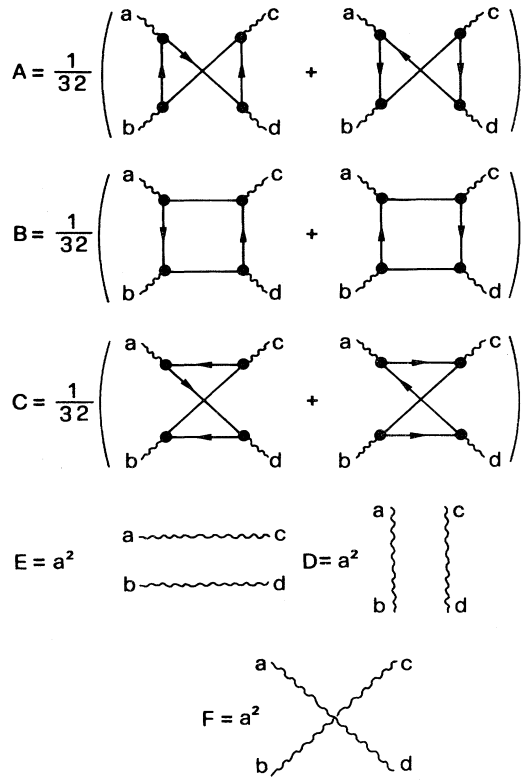

FIG. 1. A set of tensors that form a "natural" basis for rank-four tensors. Their analytic definition is in (2.3). Wavy lines represent particles in the adjoint representation, solid straight lines are in the fundamental representation.

In the evaluation of the group factor of a given graph G it is useful to consider it as a product of the group factors of two (or more) subgraphs G_1 and G_2 previously computed: $W_G = W_{G_1} W_{G_2}$.

As is well known ladder graphs (Fig. 2) are the set most relevant for the bound states (in the weak-coupling approximation for the kernel of the Bethe-Salpeter equation) and for the high-energy behavior (in the leading-log energy approximation).

To compute the group factor W_{r+1} of the ladder with $r+1$ rungs it is sufficient to project W_1 into the six channels with pure quantum numbers (Fig. 3):

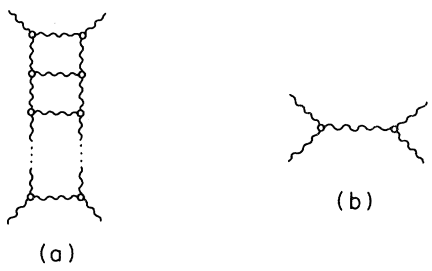

FIG. 2. (a) The ladder graph. (b) One step of the ladder graph.

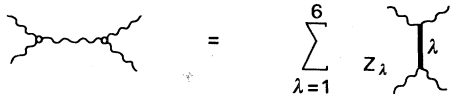

FIG. 3. Projection of the group weight of one step of the ladder graph into pure quantum numbers in the t channel.

$$W_1 = \sum_{\lambda=1}^{6} \omega_\lambda P_\lambda \ , \tag{2.6}$$

$$W_{r+1} = \left[\sum_{\lambda=1}^{6} \omega_\lambda P_\lambda \right]^{r+1} = \sum_{\lambda=1}^{6} (\omega_\lambda)^{r+1} P_\lambda \ , \tag{2.7}$$

where we used the orthonormality of the projector tensors:

$$P_i P_j = \delta_{ij} P_j \ . \tag{2.8}$$

The coefficients ω_λ are simply related to a set of generalized Wigner $6j$ coefficients, as one sees by multiplying both sides of Fig. 3 by a projector P_μ (Fig. 4), where d_μ is the dimension of the representation of the projector P_μ. We find

$$W_1 = \frac{N^2-4}{N} P_1 + \frac{N^2-4}{2N} P_2 + \frac{N^2-12}{2N} P_3 + \left[-\frac{2}{N} \right] P_4 + \frac{N-2}{N} P_5 - \frac{N+2}{N} P_6 \ . \tag{2.9}$$

The high-energy (large-s), fixed-momentum-transfer (fixed-t) behavior of the space-time factor of a ladder graph with $r+1$ rungs is well known:[5]

$$f_{r+1}(s,t) \sim g^2 \frac{[g^2 K(t) \ln s]^r}{s r!} \ , \tag{2.10}$$

where $K(t)$ is the usual bubble graph in two dimensions:

$$K(t) = \int \frac{d^2k}{(2\pi)^3} \frac{1}{(k^2+m^2)[(\Delta-k)^2+m^2]} \ , \qquad \Delta^2 = -t \ . \tag{2.11}$$

We now consider the "twisted" ladder graph where the variables s and u are exchanged. Its group weight is

$$W_{r+1} = \sum_{i=1}^{6} c_i (\omega_i)^{r+1} P_i \ , \tag{2.12}$$

where $c_i = +1$ for the symmetric channels $i = 1,3,5,6$, and $c_i = -1$ for the antisymmetric channels $i = 2,4$.

By considering together the space-time part and the group factor we may read our perturbative result as the weak-coupling expansion of six signatured Regge poles

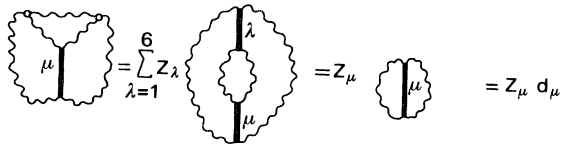

FIG. 4. The relation between the coefficients ω_μ and a set of Wigner $6j$ coefficients.

$$F(s,t)=\sum_{i=1,3,5,6}\beta_i[1+e^{-i\pi\alpha_i(t)}]s^{\alpha_i(t)}P_i + \sum_{i=2,4}\beta_i[1-e^{-i\pi\alpha_i(t)}]s^{\alpha_i(t)}P_i \ . \tag{2.13}$$

The trajectories and residues of the four even-signatured amplitudes are

$$\begin{aligned}
&\beta_1=g^2\frac{N^2-4}{N},\quad \alpha_1=-1+g^2\left[\frac{N^2-4}{N}\right]K(t)\ ,\\
&\beta_3=g^2\frac{N^2-12}{2N},\quad \alpha_3=-1+g^2\left[\frac{N^2-12}{2N}\right]K(t)\ ,\\
&\beta_5=g^2\frac{N-2}{N},\quad \alpha_5=-1+g^2\left[\frac{N-2}{N}\right]K(t)\ ,\\
&\beta_6=-g^2\frac{N+2}{N},\quad \alpha_6=-1-g^2\left[\frac{N+2}{N}\right]K(t)\ .
\end{aligned} \tag{2.14}$$

The trajectories and residues of the two odd-signatured amplitudes are

$$\begin{aligned}
&\beta_2=g^2\frac{N^2-4}{2N},\quad \alpha_2=-1+g^2\left[\frac{N^2-4}{2N}\right]K(t)\ ,\\
&\beta_4=-g^2\frac{2}{N},\quad \alpha_4=-1-g^2\left[\frac{2}{N}\right]K(t)\ .
\end{aligned} \tag{2.15}$$

III. REGGE CUTS

In this section we study the high-energy limit of the graphs with Regge cuts due to a pair of Regge poles being exchanged in the t channel.[6-8] In the leading-logarithmic approximation, it is only necessary to study the Mandelstam graph (Fig. 5) and the three related graphs obtained from it by twisting one or both ladders.[9] The asymptotic behavior of the Mandelstam graph with r_1+1 rungs in one ladder and r_2+1 in the other is

$$\frac{g^4}{s^3}\int\frac{d^2q}{(2\pi)^3}\frac{[g^2K(\Delta+q)\ln s]^{r_1+1}[g^2K(\Delta-q)\ln s]^{r_2+1}}{(r_1+1)!(r_2+1)!}\ . \tag{3.1}$$

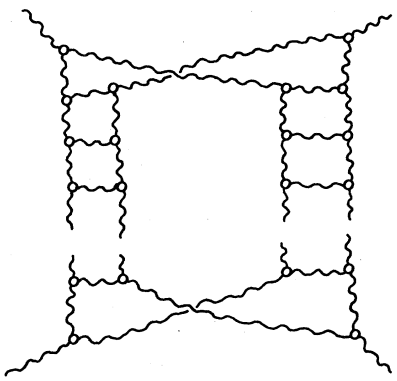

FIG. 5. The Mandelstam graph.

It is necessary to study the group factor of the Mandelstam graph. Since we are interested in the group factor for arbitrary values of the number of rungs r_1 and r_2, the group factor of each ladder is first decomposed into projectors (2.9). One is then led to compute the set of tensors $M_{\mu\nu}$ $(\mu,\nu=1,\ldots,6)$ which are the weight factors of the Mandelstam graph where the ladders have been replaced by the projectors P_μ, P_ν (Fig. 6).

A. The group factors

The tensors $M_{\mu\nu}$ may themselves be written in terms of the usual projectors (Fig. 6):

$$M_{\mu\nu}=\sum_{\sigma=1}^{6}m^\sigma_{\mu\nu}P^\sigma\ . \tag{3.2}$$

Although it only involves elementary algebra, the explicit evaluation of $M_{\mu\nu}$, or its coefficients $m^\sigma_{\mu\nu}$, requires much work and it is the main contribution of the present paper. When $M_{\mu\nu}$ is know, the group weight of the generic Mandelstam graph $W_M(r_1+1,r_2+1)$ is also known. By use of (2.9) we find

$$W_M(r_1+1,r_2+1)=\sum_{\sigma=1}^{6}P^\sigma\sum_{\mu,\nu=1}^{6}(\omega_\mu)^{r_1+1}(\omega_\nu)^{r_2+1}m^\sigma_{\mu\nu}\ . \tag{3.3}$$

Because of the symmetry of the cubic coupling and the symmetry of the graph in Fig. 6 one has

$$m^\sigma_{\mu\nu}=m^\sigma_{\nu\mu},\quad \mu,\nu,\sigma=1,2,\ldots,6\ . \tag{3.4}$$

By multiplying both sides of Eq. (3.2) by the projector P^λ and by saturating the remaining indices we see that $m^\sigma_{\mu\nu}$ are simply related to the most nonplanar type of generalized Wigner $15j$ coefficients (Fig. 7).

Before quoting our results for the tensor $M_{\mu\nu}$, we list some symmetry properties and special values for the coefficients $m^\sigma_{\mu\nu}$.

(1) In Fig. 7 one has

$$(m^\lambda_{\mu\nu})d_\lambda=(m^\nu_{\mu\lambda})d_\nu=(m^\mu_{\lambda\nu})d_\mu\ , \tag{3.5}$$

where the repeated index is not summed.

(2) Because of the symmetry of the Mandelstam graph,

$$M^\sigma_{\mu\nu}=0 \tag{3.6}$$

if one or three of the indices correspond to antisymmetric projectors.

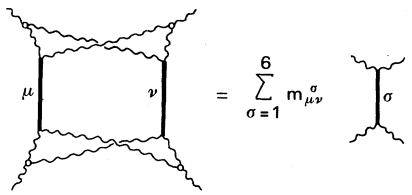

FIG. 6. Graphical representation for the definition of the coefficients $m^\sigma_{\mu\nu}$ in (3.2).

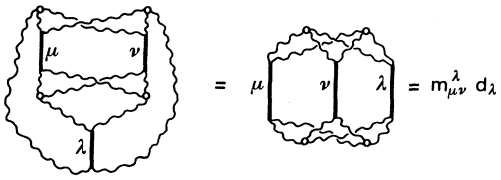

FIG. 7. The relation between the coefficients $m^{\lambda}_{\mu\nu}$ and a set of Wigner $15j$ coefficients.

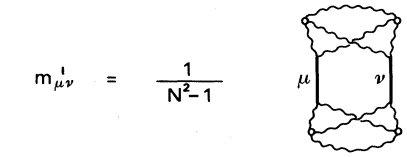

FIG. 8. The special case of the coefficient $m^{\lambda}_{\mu\nu}$ for one of the indices corresponding to the projector P_1 of the singlet representation.

(3) If one index corresponds to the projector of the singlet representation, $m^{\sigma}_{\mu\nu}$ is computable from the generalized Wigner $6j$ coefficients (2.6). As shown in Fig. 8,

$$m^{1}_{\mu\nu}=\frac{\delta_{\mu\nu}}{N^2-1}(\omega_\mu)^2 d_\mu \tag{3.7}$$

(where the repeated index is not summed), next by use of (3.5)

$$m^{\nu}_{1\mu}=\frac{\delta_{\mu\nu}}{N^2-1}(\omega_\mu)^2 . \tag{3.8}$$

(4) By summing one index on the range of its possible values, for instance, the two antisymmetric projectors, or the four symmetric ones, its representation is replaced by the identity in the antisymmetric space or in the symmetric space. Then one-index sums of $m^{\sigma}_{\mu\nu}$ are expressed by certain generalized Wigner $12j$ coefficients. Two index sums are given by simple $9j$ coefficients proportional to the dimension of the remaining representation (Fig. 9). For instance,

$$\sum_{\mu,\nu=1,3,5,6}(m^{2}_{\mu\nu})d_\lambda=\frac{(N^2-4)^2}{N^2}d_\lambda , \tag{3.9}$$

λ not summed.

(5) $N\to -N$ symmetry. The symmetric projectors P_5 and P_6 are related under the exchange $N\to -N$, as we show in the Appendix. Then we obtain[11]

$$[d_5(m^{5}_{\mu\nu})]_{SU(N)}=[(m^{6}_{\mu\nu})d_6]_{SU(-N)} \tag{3.10}$$

and

$$(m^{5}_{\mu\nu})_{SU(N)}=(m^{6}_{\mu\nu})_{SU(-N)} . \tag{3.11}$$

Because of Eq. (3.6) $M_{\mu\nu}$ has nonvanishing coefficients only for projectors P^{σ} with definite symmetry (all of them symmetric or all of them antisymmetric). We quote the results of the antisymmetric terms in Table I and the symmetric terms in Table II.

The reading of Tables I and II is illustrated by the following examples:

$$M_{23}=\frac{4}{N^2}P_2+\frac{(N^2-8)^2}{4N^2(N^2-4)}P_4 +0P_1+0P_3+0P_5+0P_6 , \tag{3.12}$$

$$M_{24}=0P_1+\frac{(N^2-8)^2}{8N^2}P_3+\frac{(N-2)(N+1)}{2N^2}P_5 +\frac{(N+2)(N-1)}{2N^2}P_6+0P_2+0P_4 .$$

TABLE I. List of the tensors $M_{\mu\nu}$ that have nonvanishing components with the antisymmetric projectors (P_2 and P_4).

Tensor	P_2 projection	P_4 projection
M_{12}	$\frac{(N^2-4)^2}{4N^2(N^2-1)}$	0
M_{14}	0	$\frac{4}{N^2(N^2-1)}$
M_{23}	$\frac{4}{N^2}$	$\frac{(N^2-8)^2}{4N^2(N^2-4)}$
M_{25}	$\frac{(N-2)^2(N+3)}{16(N+1)}$	$\frac{(N+3)}{4(N+2)}$
M_{26}	$\frac{(N+2)^2(N-3)}{16(N-1)}$	$\frac{(N-3)}{4(N-2)}$
M_{34}	$\frac{(N^2-8)^2}{8N^2}$	$\frac{(N^2-8)(N^2+16)}{2N^2(N^2-4)}$
M_{45}	$\frac{(N-2)(N+3)}{8}$	$\frac{(2N^3+3N^2-17N-10)(N+3)}{8(N+2)(N+1)}$
M_{46}	$\frac{(N+2)(N-3)}{8}$	$\frac{(2N^3-3N^2-17N+10)(N-3)}{8(N-2)(N-1)}$

TABLE II. List of the tensors $M_{\mu\nu}$ that have nonvanishing components with the symmetric projectors (P_1, P_3, P_5, P_6).

Tensor	P_1 projection	P_3 projection	P_5 projection	P_6 projection
M_{11}	$\frac{(N^2-4)^2}{N^2(N^2-1)}$	0	0	0
M_{13}	0	$\frac{(N^2-12)^2}{4N^2(N^2-1)}$	0	0
M_{15}	0	0	$\frac{(N-2)^2}{N^2(N^2-1)}$	0
M_{16}	0	0	0	$\frac{(N+2)^2}{N^2(N^2-1)}$
M_{22}	$\frac{(N^2-4)^2}{4N^2}$	$\frac{4}{N^2}$	$\frac{(N-2)^2}{4N^2}$	$\frac{(N+2)^2}{4N^2}$
M_{24}	0	$\frac{(N^2-8)^2}{8N^2}$	$\frac{(N-2)(N+1)}{2N^2}$	$\frac{(N+2)(N-1)}{4N^2}$
M_{33}	$\frac{(N^2-12)^2}{4N^2}$	$\frac{16(N^2-10)^2}{N^2(N^2-4)^2}$	$\frac{(N^2+4N-8)^2}{4N^2(N+2)^2}$	$\frac{(N^2-4N-8)^2}{4N^2(N-2)^2}$
M_{35}	0	$\frac{(N+3)(N^2+4N-8)^2}{16(N+1)(N+2)^2}$	$\frac{(N+1)(N-4)(N^2-16)}{2N^2(N+2)^2}$	0
M_{36}	0	$\frac{(N-3)(N^2-4N-8)^2}{16(N-1)(N-2)^2}$	0	$\frac{(N-1)(N+4)(N^2-16)}{2N^2(N-2)^2}$
M_{44}	$\frac{2(N^2-4)}{N^2}$	$\frac{(N^2+16)(N^2-8)}{4N^2}$	$\frac{(N-2)(2N^3+3N^2-17N-10)}{4N^2}$	$\frac{(N+2)(2N^3-3N^2-17N+10)}{4N^2}$
M_{55}	$\frac{(N-2)^2(N+3)}{4(N+1)}$	$\frac{(N+4)(N-4)^2(N+3)}{8(N+2)^2}$	$\frac{(N-2)(N-1)(5N^3+48N^2+145N+126)}{16(N+1)(N+2)^2}$	$\frac{(N+1)(N+3)}{16}$
M_{56}	0	0	$\frac{(N+1)^2(N-3)}{16(N-1)}$	$\frac{(N-1)^2(N+3)}{16(N+1)}$
M_{66}	$\frac{(N+2)^2(N-3)}{4(N-1)}$	$\frac{(N-4)(N+4)^2(N-3)}{8(N-2)^2}$	$\frac{(N-1)(N-3)}{16}$	$\frac{(N+2)(N+1)(5N^3-48N^2+145N-126)}{16(N-2)^2(N-1)}$

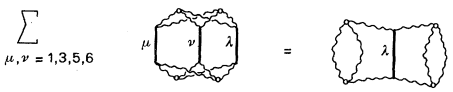

FIG. 9. Representation of Eq. (3.9).

B. Putting together space-time and group factors

Let us consider a Mandelstam graph where one of the ladders is twisted. The space-time factor is the opposite[7,8] of that in Eq. (3.1), while the group factor contributes a term $+1$ when a symmetric projector is twisted and -1 when an antisymmetric projector is twisted. The sum of all the leading logarithms contributing to the two-Reggeon cut is conveniently written as a superposition of contributions in symmetric channels and in antisymmetric channels:

$$F(s,t)=F_S(s,t)+F_A(s,t)\ , \tag{3.13}$$

$$F_S(s,t)=\sum_{k=1,3,5,6} F^{(k)}(s,t)P^k\ , \tag{3.14}$$

$$F_A(s,t)=\sum_{k=2,4} F^{(k)}(s,t)P^k\ , \tag{3.15}$$

where

$$F^{(k)}(s,t)=\frac{1}{s}\sum_{i,j=2,4} c_{ij}^k\int\frac{d^2q}{(2\pi)^2}\beta_i(\Delta+q)(1-e^{-i\pi\alpha_i(\Delta+q)})s^{\alpha_i(\Delta+q)}\beta_j(\Delta-q)(1-e^{-i\pi\alpha_j(\Delta-q)})s^{\alpha_j(\Delta-q)} \tag{3.16}$$

if $k=1,3,5,6$ and

$$F^{(k)}(s,t)=\frac{1}{s}\sum_{\substack{i=1,3,5,6\\ j=2,4}} 2c_{ij}^k\int\frac{d^2q}{(2\pi)^2}\beta_i(\Delta+q)(1+e^{-i\pi\alpha_i(\Delta+q)})s^{\alpha_i(\Delta+q)}\beta_j(\Delta-q)(1-e^{-i\pi\alpha_j(\Delta-q)})s^{\alpha_j(\Delta-q)} \tag{3.17}$$

if $k=2,4$.

The coefficients c_{ij}^k measure the couplings of two Reggeons to the two external particles

$$c_{ij}^k\equiv g^4\frac{m_{ij}^k}{\beta_i\beta_j}\ . \tag{3.18}$$

The residues $\beta(t)$ and trajectories are still given by (2.11) and (2.12).

Equations (3.16) and (3.17) show that the leading contribution in antisymmetric channels is due to the convolution of one symmetric Reggeon with an antisymmetric one, while in the symmetric channels it is due to the convolution of two antisymmetric ones. Of course one would expect, in the symmetric channels, also the contribution due to the convolution of two symmetric Reggeons. We have not quoted it because, as one may easily check by expanding in perturbation theory, its contribution is suppressed by a factor $(\log s)^2$ with respect to the contributions (3.16), due to the signature factor.

IV. CONCLUSIONS

This model may be considered the well-studied scalar cubic interaction, dressed up with an internal symmetry group, and its dynamics is predictably close to that of the latter. In the six channels with definite quantum numbers ($\mu=1,\ldots,6$) one finds Regge poles of the usual form: their trajectories computed in perturbation expansion is

$$\alpha_\mu(t)=-1+g^2c_\mu K(t)+O(g^4)\ . \tag{4.1}$$

However, because of the presence of the internal symmetry, two channels ($\mu=2,4$) are antisymmetric; there does not occur cancellation of leading logarithms related to the signature factor of the symmetric (even-signatured) channels. Indeed the leading logarithms in the antisymmetric channels sum up to produce odd-signatured Regge poles.

A similar situation occurs for the two-Reggeon cut. In leading order only the Mandelstam graph and the three graphs related to it by twisting a ladder may contribute. Because of the symmetry of the nonplanar subgraph that couples the two ladders to the two external particles, the two-Reggeon cut originated by the exchange of two Regge poles with the same symmetry properties (both even signatured or both odd) only contributes to the symmetric channels while the exchange of two Regge poles with different signatures only contributes to the antisymmetric channels.

The major effort in this work was the computation of the couplings between the two Regge poles and the two external particles, given by the coefficients $m_{\mu\nu}^\lambda$ in (3.2) or c_{ij}^k in (3.18). Of course they are model dependent but the technique used in computing them will certainly be useful for any other model. Their numerical values may also be suggestive, particularly if it will be possible to interpret them merely in terms of the dimensions of the representation involved. In this sense Fig. 7 is rather promising, because the nonplanar coupling that appears there is actually the simplest possible way to couple three representations.

It may be interesting to consider the large-N, fixed $g^2N\equiv\gamma^2$ limit of this model. Only the first three Regge poles survive:

$$\beta_1=\gamma^2,\quad \alpha_1=-1+\gamma^2K(t)\ , \tag{4.2}$$

$$\beta_3=\tfrac{1}{2}\gamma^2,\quad \alpha_3=-1+\tfrac{1}{2}\gamma^2K(t)\ , \tag{4.3}$$

$$\beta_2=\tfrac{1}{2}\gamma^2,\quad \alpha_2=-1+\tfrac{1}{2}\gamma^2K(t)\ , \tag{4.4}$$

while the other three Regge poles have vanishing residues and flat trajectories in this limit. This could not be antici-

pated by the usual dominance of planar graphs since all the six Regge poles come from the ladder graphs. Analogous simpler formulas are obtained for the couplings of two Regge poles into a Regge cut. The only nonvanishing couplings $m^{\lambda}_{\mu\nu}$ with $\mu,\nu=1,2,3$ are

$$m^{1}_{22}=m^{1}_{33}=\frac{N^2}{4}\ , \tag{4.5}$$

$$m^{2}_{12}=m^{2}_{13}=m^{5}_{22}=m^{6}_{22}=m^{5}_{33}=m^{6}_{33}=m^{1}_{23}=\tfrac{1}{4}\ , \tag{4.6}$$

$$m^{1}_{11}=1\ . \tag{4.7}$$

Then in the large-N limit the only nonvanishing two-Reggeon-cut contributions are in the singlet channel and they are due to the exchange of two Regge poles $\alpha_2(t)$ or two Regge poles $\alpha_3(t)$. These contributions are just of the same order in N of the singlet Regge pole:

$$F(s,t)P_1=P_1\beta_1(t)s^{\alpha_1(t)}+P_1\frac{1}{4s}\left[\int\frac{d^2q}{(2\pi)^2}\beta_2(1-e^{-i\pi\alpha_2(\Delta+q)})s^{\alpha_2(\Delta+q)}\beta_2(1-e^{-i\pi\alpha_2(\Delta-q)})s^{\alpha_2(\Delta-q)}\right.$$
$$\left.+\frac{1}{s}\int\frac{d^2q}{(2\pi)^2}\beta_3(1+e^{-i\pi\alpha_3(\Delta+q)})s^{\alpha_3(\Delta+q)}\beta_3(1+e^{-i\pi\alpha_3(\Delta-q)})s^{\alpha_3(\Delta-q)}\right]. \tag{4.8}$$

It might be surprising that the Mandelstam graph, which contains two nonplanar insertions, is of the same order of the Regge pole for large N. This indeed may occur only for its projection in the singlet channel, which is given by a planar graph [see Figs. 10(a) and 10(b)].

Presumably the present analysis may have some value in setting up hybrid models where Regge poles replace ladder graphs. Let us consider, for instance, a hybrid model with just one Regge pole, that one belonging to the channel of the adjoint representation (here indicated by the projector P_2). Notice that such a hybrid model would not be far from the present one in the sense that from a strictly leading-logarithm analysis only Regge poles in the two antisymmetric channels would emerge, because of the above-mentioned cancellations occurring in symmetric channels. Furthermore, in the large-N limit, with g^2N fixed, the Regge pole in the P_4 channel would be depressed while the P_2 Regge pole would not. To have a closer comparison with the analysis of SU(N) gauge theory one may assume that only one Regge pole has a trajectory originating at $J=1$:

$$\alpha_2(t)=1+g^2c_2K(t)+O(g^4)\ . \tag{4.9}$$

The main qualitative features that would emerge are the following:

There is no contribution of the two-Reggeon cut in the channel of the adjoint representation, because of the vanishing of m^{2}_{22}.

For the same reason there would be neither a Regge pole nor a two-Reggeon cut in the second antisymmetric channel (the P_4 channel).

There would be no Regge pole, but only two-Reggeon-cut contributions in the four symmetric channels.

These features bear some similarity with the present understanding[12] of SU(N) gauge theories.

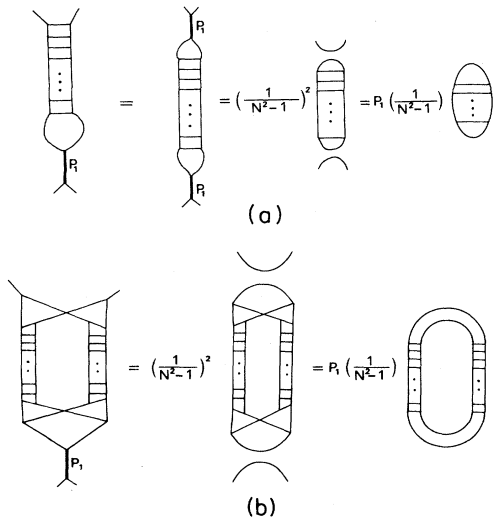

FIG. 10. (a) The projection of the group weight of the ladder graph into the singlet channel. (b) The projection of the group weight of the Mandelstam diagram into the singlet channel. For an easier drawing here, as well as in (a), the thin smooth lines represent particles in the adjoint representation while in Figs. 1 to 9 these are represented by wavy lines.

APPENDIX

The simplest way to exhibit the relation between P_5 and P_6 is to exhibit them in graphical form as states with two quarks and two antiquarks.

For this appendix only, "multiplication" of tensors is defined in a horizontal way.

We find

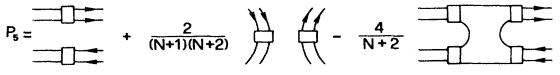

(A1)

(A2)

where the open (solid) boxes mean symmetrization (antisymmetrization).

Let us now consider the generalized Wigner $15j$ coefficient $(m^5_{\mu\nu})d_5$ (see Fig. 7). It can be computed as the sum of three contributions as shown in (A1). In the first two contributions one may replace symmetrization boxes with antisymmetrization ones and one obtains contributions equal to the previous, after the replacement $(N \to -N)$.

The third contribution of Eq. (A1) has different parity of boundaries and, when the exchange of open boxes into solid boxes is performed, produces the opposite result than the replacement $N \to -N$. However this different behavior just compensates the explicit coefficients in (A1) and (A2), thus proving Eq. (3.10).[11,13]

---

[1]P. Cvitanović, Phys. Rev. D 14, 1536 (1975), and book in progress.

[2]These basis tensors were already used in P. Butera *et al.*, Phys. Rev. D 21, 972 (1980), where a table of their "products" was also given, together with the relations with the projector basis. Notice, however, that we inserted a factor a^2 in the present definition of D,E,F to obtain a homogeneous dependence of the projectors on the normalization (2.5), and a further factor $\frac{1}{16}$ in the definition of A,B,C.

[3]The two conjugate representations of dimension $\frac{1}{4}(N^2-4)(N^2-1)$ appear together, so there is no need to introduce a seventh basis tensor

$$A_{abcd} \equiv \frac{1}{32}[\mathrm{Tr}(\lambda_a\lambda_d\lambda_c\lambda_b) - \mathrm{Tr}(\lambda_a\lambda_b\lambda_c\lambda_d)]$$

to "resolve" them. Even if the Lagrangian (1.1) is modified by adding fermionic fields in the fundamental representation, the space-time factors are related by the Furry theorem and the "natural" basis tensors (2.3) or the projector basis (2.5) are still complete.

[4]For $N=3$ the Macfarlane *et al.* relation yields $P_6=0$: A. J. Macfarlane *et al.*, Commun. Math. Phys. 11, 77 (1978).

[5]See, for instance, R. Eden *et al.*, *The Analytic S-Matrix* (Cambridge University Press, Cambridge, England, 1966).

[6]The original works for Regge cuts in perturbation theory are S. Mandelstam, Nuovo Cimento 30, 1148 (1963); J. C. Polkinghorne, J. Math. Phys. 4, 1396 (1963). A review is in Ref. 5.

[7]The first correct evaluation of the space-time factor of the Mandelstam graph is given in G. M. Cicuta and R. L. Sugar, Phys. Rev. D 3, 970 (1971) and B. Hasslacher and D. K. Sinclair, *ibid.* 3, 1770 (1971). The computation was checked by a number of authors (Ref. 8).

[8]I. G. Halliday and C. T. Sachrajda, Phys. Rev. D 8, 3598 (1973); A. R. Swift, *ibid.* 5, 1400 (1972).

[9]For simplicity we only study the graphs with only one large rapidity gap. It is well known that graphs with more than one large rapidity gap, usually interpreted as iterations in the t channel or many-body forces, are relevant both in perturbation theory, and for the whole behavior of the model. See, for instance, Ref. 10.

[10]B. M. McCoy and T. T. Wu, Phys. Rev. D 12, 546 (1975); 12, 578 (1975); A. R. Swift, Nucl. Phys. B84, 397 (1975); H. D. I. Abarbanel *et al.*, Phys. Rep. 21C, 120 (1975).

[11]This exact equation has been discovered by P. Cvitanović in discussion and collaboration with the authors.

[12]The proper list of references would be rather long. Here are only a few that allow us to find the others: M. T. Grisaru, H. J. Schnitzer, and H. S. Tsao, Phys. Rev. D 8, 4498 (1973); B. M. McCoy and T. T. Wu, *ibid.* 13, 1076 (1976); L. N. Lipatov, Yad. Fiz. 23, 642 (1976) [Sov. J. Nucl. Phys. 23, 338 (1976)]; H. Cheng and C. Y. Lo, Phys. Rev. D 15, 2959 (1977); J. B. Bronzan and R. L. Sugar, *ibid.* 17, 585 (1978); L. Lukaszuk and L. Szymanowski, Nucl. Phys. B159, 316 (1979); J. Bartels, *ibid.* B151, 293 (1979).

[13]P. Cvitanović and A. D. Kennedy, Phys. Scr. 26, 5 (1982); R. L. Mkrtchyan, Phys. Lett. 105B, 174 (1981).